01 Jul 2017

# Effects of specimen size and yttria concentration on mechanical properties of single crystalline yttria-stabilized tetragonal zirconia nanopillars

Ning Zhang

Mohsen Asle Zaeem
*Missouri University of Science and Technology*, zaeem@mst.edu



## Recommended Citation

N. Zhang and M. Asle Zaeem, "Effects of specimen size and yttria concentration on mechanical properties of single crystalline yttria-stabilized tetragonal zirconia nanopillars," *Journal of Applied Physics*, vol. 122, no. 1, American Institute of Physics (AIP), Jul 2017.
The definitive version is available at https://doi.org/10.1063/1.4991339

# Effects of specimen size and yttria concentration on mechanical properties of single crystalline yttria-stabilized tetragonal zirconia nanopillars

Ning Zhang and Mohsen Asle Zaeem[a)]
*Department of Materials Science and Engineering, Missouri University of Science and Technology, Rolla, Missouri 65409, USA*

(Received 3 April 2017; accepted 20 June 2017; published online 6 July 2017)

The nanoscale plastic deformation of yttria-stabilized tetragonal zirconia (YSTZ) is highly dependent on the crystallographic orientations, i.e., dislocation is induced when the loading direction is 45° tilted to {111} and {101} slip planes, while tetragonal to monoclinic phase transformation dominates the plastic deformation when loading direction is perpendicular to the slip planes. This study investigates the effects of specimen size and yttria concentration on the mechanical response of single crystalline YSTZ nanopillars. Through uniaxial compression test, the smaller-is-stronger phenomenon is revealed in nanopillars deformed through a dislocation motion mechanism. Serrated stacking faults are observed in the smallest nanopillar, while neat primary slip plane forms in the largest nanopillar. In contrast, the larger-is-stronger relation is observed in nanopillars in which deformation is mediated by tetragonal to monoclinic phase transformation. It is noted that the ratio of transformed monoclinic phase to the remaining tetragonal phase is the highest in the smallest nanopillar. The strength of nanopillars is identified to decrease by increasing the amount of yttria due to the creation of more oxygen vacancies that act as weak points to facilitate dislocation motion and accelerate phase transformation. *Published by AIP Publishing.*
[http://dx.doi.org/10.1063/1.4991339]

## I. INTRODUCTION

Stabilized tetragonal zirconia has become one of the industrially important ceramic materials because of its high-strength, low thermal conductivity, high corrosion resistance, and high ionic conductivity. Zirconia exists in three crystalline polymorphs, namely, monoclinic (<1430 K), tetragonal (1430–2640 K), and cubic (>2640 K).[1] Of particular interest is the martensitic transformation from tetragonal to monoclinic phase ($t \rightarrow m$) of zirconia,[2] which is greatly important for mechanical and structural applications, because it is the basis for transformation toughening[3] and shape memory applications.[4]

Tetragonal zirconia can be stabilized at room temperature by adding suitable oxides such as yttria ($Y_2O_3$).[5] In a recent study, by means of molecular dynamics (MD) simulations, it was demonstrated that yttria-stabilized tetragonal zirconia (YSTZ) exhibits a pronounced plastic anisotropic property.[6] Various deformation mechanisms including dislocation motion, phase transformation, and a combination of dislocation motion and phase transformation were revealed under uniaxial compression along different orientations. In a recent experimental study,[7] such crystal orientation dependence of martensitic transformation in zirconia-based shape memory ceramic was also reported. Besides orientations, other factors can also affect the mechanical properties, such as specimen size and composition of the material.

Many materials exhibit strong size effect at the micro- and sub-micro scale, especially at nanometer length scale. Various studies have evidenced that material strength increases as the sample dimension decreases within a certain nanometer size range.[8,9] To date, studies on single crystalline,[10–12] nanocrystalline,[13–16] precipitate-strengthened,[17] and nanoporous[18] metals have demonstrated that the mechanical strength of the metals is directly related to the grain size and the sample size. Considering the extrinsic specimen size effect, different deformation and strengthening mechanisms were identified for different small scale materials. For example, hardening by dislocation starvation was identified in nanoscale gold nanopillar,[19] and a brittle-to-ductile transition in silicon nanopillar was observed when nanopillar diameter decreases from 400 nm to 310 nm.[20] Moreover, some experimental efforts have been dedicated to study the extrinsic size effect in micro and sub-micrometer pillar ceramics, especially in zirconia pillars. TEM inspection of zirconia particles revealed that the crystal structure is strongly dependent on their size.[21] In recent studies, it was shown that by reducing the sample size to submicron scale, cracks can be suppressed in normally brittle martensitic ceramics, such as zirconia.[22,23] Furthermore, the transformation-induced plasticity of polycrystalline tetragonal zirconia micropillars was also shown to be size dependent.[24] In the compression test of polycrystalline tetragonal zirconia micropillars, considerable compressive strength and four times larger failure strain than that in macroscopic tests were obtained.[24] Whereas, in comparison to micropillars, at nanoscale, an increase of critical stress to induce the superelastic effect and a decrease of the stress for final recovery of the reverse transformation were identified.[25] Although there is recent and ongoing progress made to study the grain and sample size effects in stabilized zirconia, a study dedicated to investigate the size effect on mechanical response of

a)Author to whom correspondence should be addressed: zaeem@mst.edu

single crystal zirconia nanopillars, in particular, to understand the underlying governing mechanisms has not been conducted yet. This is a difficult task for experiments to achieve because of the possible combinations of dislocation and phase transformation that can mediate the deformation of zirconia nanopillars,[6] and also because experiments are unable to capture the dynamic process of nanostructural evolution.

In addition to the size effect, another key factor affecting the mechanical properties of stabilized zirconia is the composition, i.e., the amount of stabilizer ($Y_2O_3$). It is well known[26–28] that at room temperature undoped zirconia has a monoclinic structure; by increasing the dopant's concentration, the material transforms to a tetragonal form, which is called partially stabilized zirconia; by doping with more than 17 mol. % $YO_{1.5}$ (or about 9 mol. % $Y_2O_3$), the cubic phase is stabilized, which is called fully stabilized zirconia. Experimental studies have demonstrated that tetragonal zirconia doped with low yttria content, e.g., 1–4 mol. % $Y_2O_3$,[29,30] can transform to monoclinic phase. Zirconia stabilized by different percentages of $Y_2O_3$ has been revealed to show rather different properties and therefore has been used in a wide variety of applications. The first observation of superplasticity in a 3 mol. % YSTZ polycrystalline ceramic was reported by Wakai *et al.*[31] Zirconia stabilized with 2–4 mol. % of $Y_2O_3$ has been used as a structural material due to the incomparably high fracture toughness derived from the stress-induced phase transformation.[32] Fracture toughness of nanocrystalline tetragonal zirconia ceramic stabilized with 1.5 mol. % $Y_2O_3$ was measured to be much higher than that of zirconia stabilized with 3 mol. % $Y_2O_3$.[33] Masaki and Sinjo also observed a non-linear increase of fracture toughness with decreasing yttria content from 2.5 to 2.0 mol. % and achieved a maximum fracture toughness of 20 MPa $m^{1/2}$ in tetragonal zirconia stabilized with 2.0 mol. % $Y_2O_3$.[34] In particular, zirconia stabilized with 8 mol. % of $Y_2O_3$ is found to have the high ionic conductivity and thus used as a solid electrolyte. The effect of $Y_2O_3$ content on improving the catalytic performance of zirconia was also studied.[35] In general, the effect of the composition of shape memory alloys on martensitic transformation temperature[36,37] is a common popular topic. In spite of the importance of the composition effect in YSTZ, an understating of $Y_2O_3$ concentration on mechanical response of YSTZ nanopillar over a wide concentration range of $Y_2O_3$ has not been established yet.

In this study, we utilize molecular dynamics (MD) simulations to study the effects of nanopillar specimen size and stabilizer ($Y_2O_3$) concentration on the behaviors of dislocation motion and phase transformation and subsequently on the mechanical response of YSTZ nanopillars.

## II. MODEL AND SIMULATION DETAILS

Atomic-level simulation approaches have played a crucial role in understanding the detailed atomic evolution of dislocation motion and phase transformation in various materials.[6,8,38,39] The ability of MD simulations to produce trustable data is essentially dependent on the reliability of the interatomic potentials. Thus, a transferable interatomic potential is required to simulate phase transformation between tetragonal and monoclinic phase of stabilized zirconia. In this study, we use the combination of short-range Born-Meyer-Buckingham (BMB) potential and the long-range Coulomb potential,[40] which was employed in the earlier studies of plastic deformation of YSTZ nanopillars[6] and has been demonstrated to be capable of capturing dislocation dynamics and $t \rightarrow m$ phase transformation simultaneously. The functional form of the potential and the parameters were given by

$$E_{ij} = \frac{q_i q_j}{r_{ij}} + A_{ij} \exp\left(-\frac{r_{ij}}{\rho}\right) - \frac{C}{{r_{ij}}^6}, \tag{1}$$

where $q_i$ and $q_j$ are the ionic charges of ions $i$ and $j$, while $A_{ij}$, $\rho$, and $C$ are potential parameters, as listed in Table I.

To build the atomic model of YSTZ, $Zr^{4+}$ cations are randomly substituted by $Y^{3+}$ ions. In order to maintain the electrical neutrality, the substitution of $Zr^{4+}$ by $Y^{3+}$ causes the formation of oxygen vacancies, which are equal to half of $Y^{3+}$ ions. All computer models of single crystalline YSTZ nanopillars have square cross sections. To study the specimen size effect, two types of representative YSTZ nanopillars whose plastic deformation are dominated by dislocation migration and phase transformation are chosen. For each type, three nanopillar models with different specimen sizes but same height-to-width ratio are generated and subjected to uniaxial compressive loading. Similarly, for the study of yttria concentration effect, YSTZ nanopillars with different deformation mechanisms are categorized. A composition range of 1–4 mol. % $Y_2O_3$ is selected. In order to comprehensively understand the governing mechanisms account for composition effect, pure tetragonal zirconia nanopillar is also generated and compressed for the purpose of making a comparison. Slip vector and coordinate number are chosen for the clear visualization of dislocation migration and phase transformation behaviors, respectively. And the output files are viewed in Tecplot, a commercial data visualization software. Free surface boundary conditions are used in all the simulations.

Our constant volume and temperature (NVT) MD simulations are performed using the open source software LAMMPS.[41] The velocity-Verlet algorithm[42] with a time step of 1 fs is used for time integration. Prior to loading, all nanopillars are fully relaxed for 0.1 ns at 298 K to reach their equilibrium by using Nose-Hoover thermostat.[43] Uniaxial

TABLE I. Interatomic potential parameters for the yttria-stabilized tetragonal zirconia (YSTZ).[40]

| Interaction | A (eV) | $\rho$ (Å) | C (eV Å$^6$) | Mass (amu) | Charge (e) |
|---|---|---|---|---|---|
| Zr-Zr | 0.0 | 1.0 | 0.0 | Zr: 91.0 | Zr: +4.0 |
| Zr-Y | 0.0 | 1.0 | 0.0 | – | – |
| Zr-O | 1453.8 | 0.35 | 0.0 | – | – |
| Y-Y | 0.0 | 1.0 | 0.0 | Y: 89.0 | Y: +3.0 |
| Y-O | 826.744 | 0.35587 | 0.0 | – | – |
| O-O | 22764.3 | 0.149 | 27.89 | O: 16.0 | O: −2.0 |

compressive deformation (displacement control) is applied on the simulated nanopillars at a constant strain rate of $1 \times 10^7$/s, which has been demonstrated to be slow enough for MD simulation[6] and no significant strain rate effect is detected. The strength of nanopillar is defined at the point where the maximum stress is reached.

## III. RESULTS AND DISCUSSION

### A. Specimen size effect: Dislocation migration

Our recent study[6] showed that [001] is one of the loading directions, in which dislocation propagation is the dominant deformation mechanism; accordingly, [001]-oriented single crystalline YSTZ nanopillars are selected to study the size effect on dislocation propagation and consequently on the mechanical properties of zirconia nanopillars. Three typical [001]-oriented small, medium, and large 3 mol. % YSTZ nanopillars are constructed, with sizes of $12.0 \times 12.0 \times 30.0\,\text{nm}^3$, $16.0 \times 16.0 \times 40.0\,\text{nm}^3$, and $20.0 \times 20.0 \times 50.0\,\text{nm}^3$, respectively. The height to width ratio of nanopillars is maintained at 2.5. Figure 1 presents the simulated stress-strain responses under compression for [001]-oriented nanopillars having different specimen sizes. As it can be seen, the three stress-strain curves show very similar deformation patterns. It is worth to clarify that the first sudden drop in stress is attributed to the initial dislocation gliding. Thereafter, a local periodicity is observed, which corresponds to the subsequent dislocation nucleation and migration. In addition, as shown in Fig. 1, the smaller the nanopillar size is, the larger the strength and yield strain are, i.e., the so-called "smaller-is-stronger" phenomenon is evident. The small-sized nanopillar shows the lowest abrupt stress drop after elastic deformation, which indicates a stronger barrier for dislocation migration. Dislocations nucleate from the sharp four edges of the nanopillar in all cases; but, the relatively high surface energy to total energy ratio of the smallest nanopillar causes its edges to be less sharp after relaxation, which consequently suppresses the emission of dislocations compared to other cases.

To disclose the reason behind the observed smaller-is-stronger phenomenon, we track the evolution of atomic

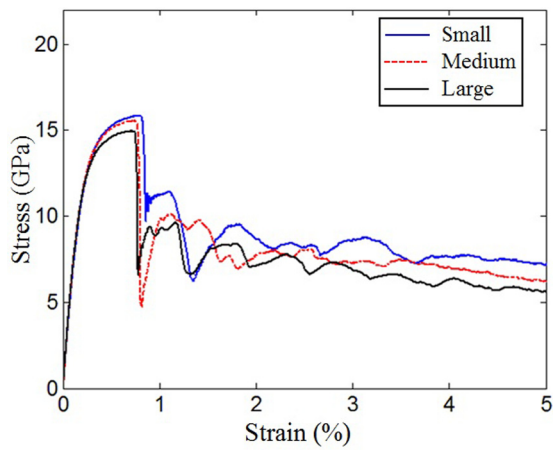


FIG. 1. Stress-strain responses of [001]-oriented zirconia nanopillars with respect to specimen size effect. The plastic deformation is dominated by dislocation migration.

structure. Slip vector is employed to clearly elucidate the process of dislocation migration (see Fig. 2). It is worth to point out that with the increase of specimen size, the ratio of surface energy to total energy becomes smaller. In other words, the smallest nanopillar has the largest surface effect. Therefore, as it can be seen in Figs. 2(a) and 2(b), serrated dislocation lines are observed in the smallest pillar and several layers of stacking faults form after gliding. By increasing strain to 1.4% and 2.0% [Figs. 2(b)–2(d)], slip plane becomes much more amorphous and thicker, and new dislocation nucleates from the surface edge of the nanopillar continuously. In addition, dislocation bifurcation is observed to accelerate energy release, as marked by black arrows in Figs. 2(b)–2(d). The primary slip system is $\{110\}$, which is also the main slip system of cubic zirconia.[44] Figures 2(b)–2(d) demonstrate that in YSTZ nanopillars with width smaller than a critical size, which is between 12 and 16 nm according to our simulation results, dislocation motion is interrupted and it is hard for a dislocation to travel through the nanopillar, which consequently results in an increase in strength and yield strain. Furthermore, this obstruction of dislocation motion leads to a higher magnitude for the local periodic peaks in the plastic flow region (see blue line in Fig. 1).

In nanopillars with medium and large specimen sizes, formation of neat primary stacking faults are observed, as presented in Figs. 2(f) and 2(j). Particularly, in the nanopillar with medium size, a secondary $\frac{1}{2}\langle 111\rangle$ partial dislocation is observed to nucleate from the edge of the nanopillar, then propagates along the primary slip plane $\{111\}$ until reaches the primary stacking fault [Figs. 2(g) and 2(h)], and this results in a lock of dislocation migration. The neat primary slip planes, as shown in Figs. 2(f)–2(h) and Figs. 2(j)–2(l), imply that the dislocation motion encounters less barrier energy and dislocation moves much easier in nanopillars having a size larger than a critical value of 16 nm; this contributes to lowering the yield stress and strain. In addition, the secondary slip planes that slightly tilts to the loading direction form with continuation of loading, which will accelerate the energy release and consequently cause the mild fluctuation of plastic stress flow (Fig. 1). Moreover, the dislocation lines show a curvy character in all the three models. However, with the increase of specimen size, the curviness of slip plane becomes less and less observable due to the decrease of surface effect. In all the cases, surface steps (or surface corrugations) are seen after dislocation migration [Figs. 2(a), 2(e), and 2(i)].

### B. Specimen size effect: Phase transformation

Besides dislocation migration, our recent study[6] also showed that, in particular, the loading directions such as $[01\bar{1}]$, phase transformation is the dominant deformation mechanism in YSTZ. Accordingly, three $[01\bar{1}]$-oriented 3 mol. % YSTZ nanopillars with sizes of $10.0 \times 10.0 \times 25.0\,\text{nm}^3$, $15.0 \times 15.0 \times 37.5\,\text{nm}^3$, and $20.0 \times 20.0 \times 50.0\,\text{nm}^3$ are generated to study the size effect on the phase transformation and mechanical response of YSTZ nanopillars under compression. The obtained stress-strain relation in Fig. 3 indicates that the larger the pillar size is, the larger the strength and yield strain are,

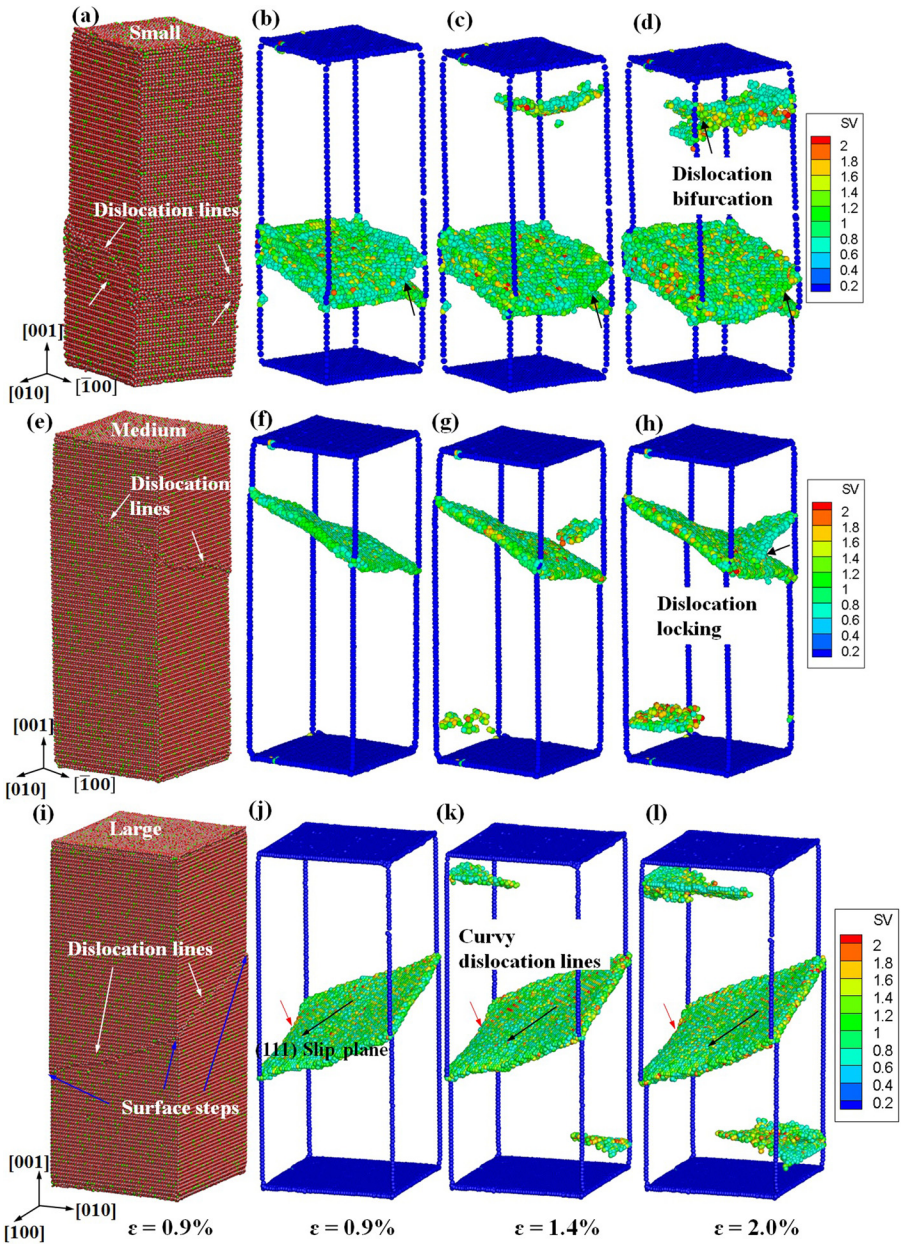


FIG. 2. 3-D atomistic snapshots of the deformed [001]-oriented small [(a)–(d)], medium [(e)–(h)], and large [(i)–(l)] zirconia nanopillars at different strains. Slip vector is employed for visualization of dislocation migration.

i.e., the so-called "larger-is-stronger" trend is observed, which is opposite to the observed "smaller-is-stronger" phenomenon in the case of size effect where dislocation migration is the dominant deformation mechanism (Fig. 1). It is worth to mention that the sudden stress drop after linear-nonlinear elastic region corresponds to the initiation of $t \rightarrow m$ phase transformation.

To reveal the reasons behind the stress-strain curves in Fig. 4, we present the atomistic structure evolutions by means of coordination number (CN). It should be noted that compared to the phase transformed configurations of medium-sized [Figs. 4(e)–4(h)] and large-sized [Figs. 4(i)–4(l)] nanopillars, the ratio of transformed monoclinic phase to the remaining tetragonal phase is much higher in the small-sized nanopillar [Figs. 4(a)–4(d)] at an equivalent strain. Furthermore, due to the significant surface effect in the smallest nanopillar at the early stage of phase transformation, the band of transformed monoclinic phase is almost parallel to the (100) top/bottom surfaces of nanopillar rather

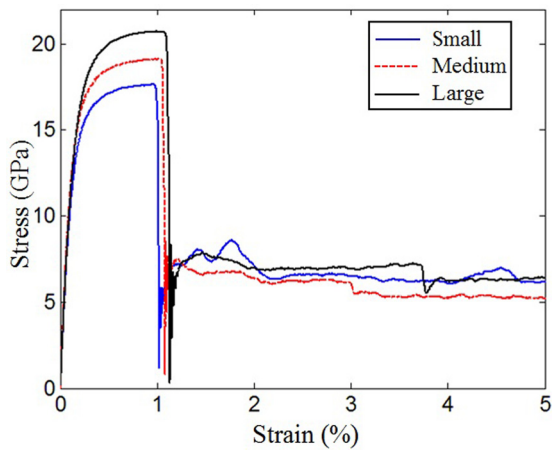


FIG. 3. Stress-strain responses of $[01\bar{1}]$-oriented zirconia nanopillars with respect to specimen size effect. The plastic deformation is dominated by phase transformation.

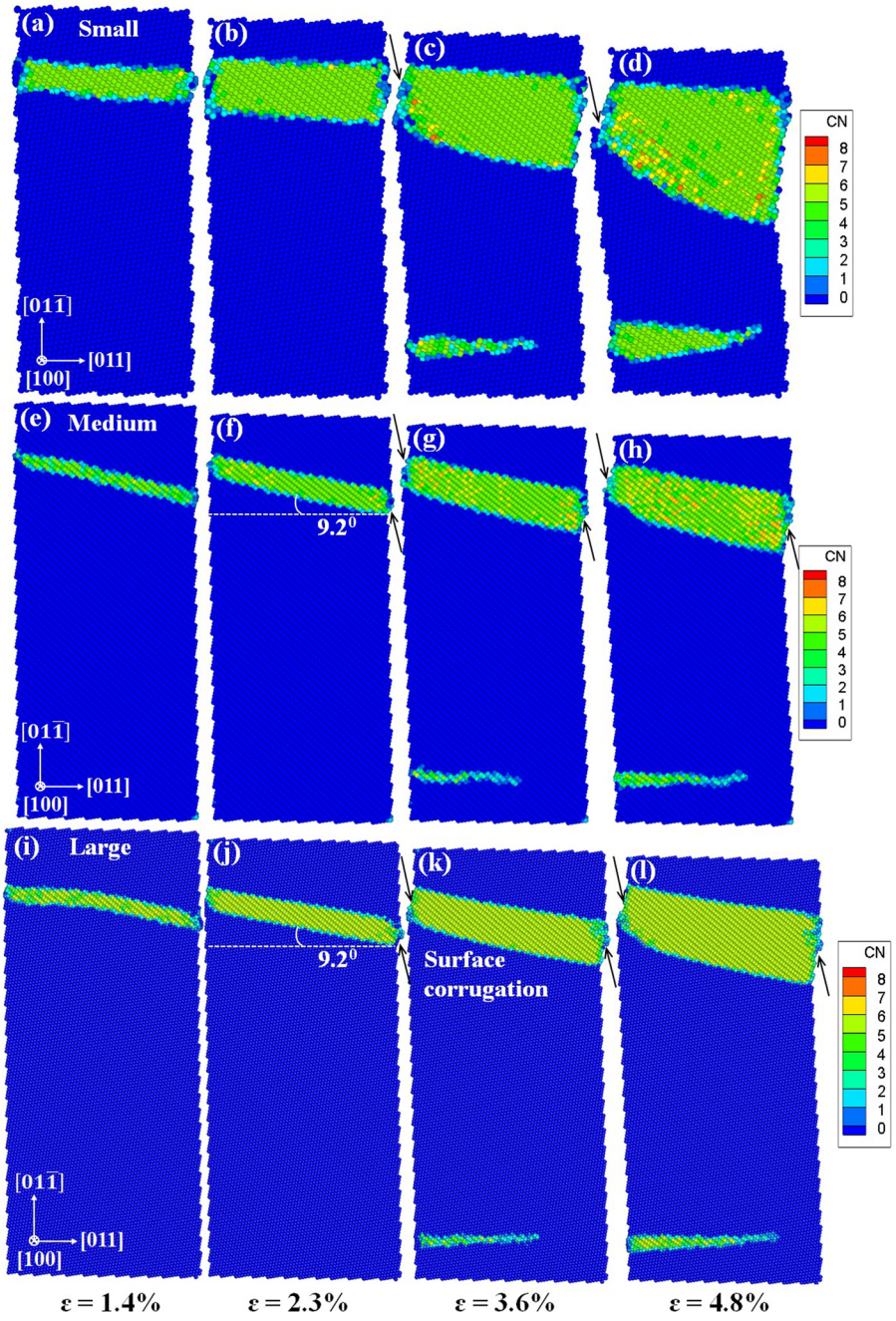


FIG. 4. Atomistic snapshots of deformed $[01\bar{1}]$-oriented YSTZ small [(a)–(d)], medium [(g) and (h)], and large [(i)–(l)] YSTZ nanopillars at different strains. Atoms are colored by CN.

than rotating an angle of ∼9.2° as observed in the medium and large nanopillars, which is in good agreement with the experimental observation.[45] Since $t \rightarrow m$ phase transformation is responsible for the plastic deformation in $[01\bar{1}]$-oriented YSTZ nanopillars, the smallest strength observed in the small-sized nanopillar (Fig. 3) is attributed to the relatively large band area of the transformed monoclinic phase. On the other hand, the transformed monoclinic phase in the medium-sized nanopillar is found to fail at a lower strain than that in the large-sized nanopillar, as indicated by orange/yellow atoms in Figs. 4(g) and 4(h). The failure of new phase implies the unstable character of the material. Therefore, the strength of medium-sized nanopillar is smaller than that of the large-sized nanopillar. Surface corrugations, as indicated by black arrows in Fig. 4, are observed in all three cases after phase transformation.

### C. Composition effect: Yttria concentration

To study the effect of composition, i.e., yttria concentration, in order to simulate tetragonal zirconia phase, [001]- and $[01\bar{1}]$- oriented YSTZ nanopillars with the following compositions are generated: 0.0 mol. % $Y_2O_3$-$ZrO_2$, 1.0 mol. % $Y_2O_3$-$ZrO_2$, 2.0 mol. % $Y_2O_3$-$ZrO_2$, 3.0 mol. % $Y_2O_3$-$ZrO_2$, and 4.0 mol. % $Y_2O_3$-$ZrO_2$, hereafter referred to as pure $ZrO_2$, 1YSTZ, 2YSTZ, 3YSTZ, and 4YSTZ, respectively. The size of all specimens is $20.0 \times 20.0 \times 47.0\,nm^3$ containing around $1.6 \times 10^6$ atoms.

To study the $Y_2O_3$ concentration effect on dislocation migration and the consequent mechanical response of YSTZ nanopillars, simulations with compressive loadings along [001] direction are conducted. The simulated stress-strain relation is plotted in Fig. 5(a). The data on strength and yield strain are extracted from Figs. 5(a) and 5(b), and the relations

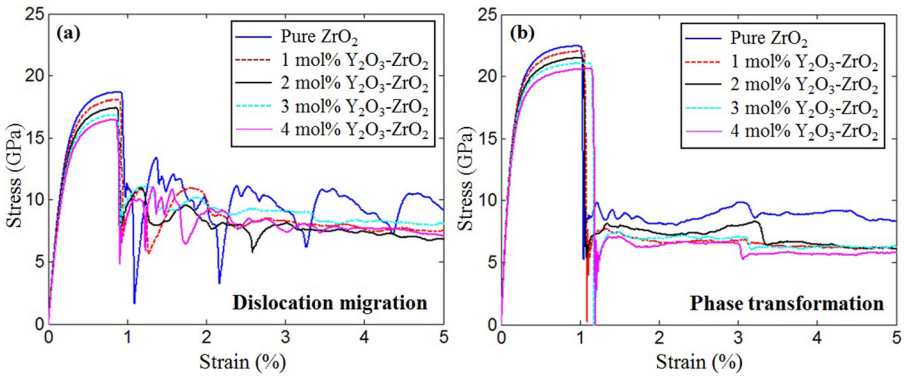


FIG. 5. Stress-strain responses of (a) [001]-oriented and (b) $[01\bar{1}]$-oriented zirconia nanopillars with respect to composition effect.

of strength versus composition and yield strain versus composition are plotted in Figs. 6(a) and 6(b), respectively. It can be seen that the nanopillars with different percentages of $Y_2O_3$ show rather different plastic deformation behaviors. Pure zirconia exhibits the highest strength and largest yield strain. With the increase of the quantity of $Y_2O_3$, the strength and yield strain become smaller and smaller. In particular, the strength of nanopillars decreases linearly with the increase of yttria concentration. Moreover, after the initial yield peak, the plastic flow stress of pure zirconia fluctuates periodically with a large magnitude, while these fluctuations in other YSTZ nanopillars show a much milder pattern. The dislocation migration trajectories colored by slip vectors at strain of 1.0% are shown in Figs. 7(a)–7(e), which manifest various dislocation gliding behaviors. In pure zirconia, clear dislocation locks are observed with each dislocation glides on different {111} slip planes [Fig. 7(a)]. This highly symmetry dislocation intersection behavior is attributed to the homogenous distribution of atoms in pure zirconia, in which once the critical stress is achieved, dislocations will be stimulated and emit from the four edges of the nanopillar almost simultaneously; then these dislocations continue to glide along the direction of highest shear stress until they meet each other and create dislocation locks in the interior of the nanopillar. This kind of dislocation locking will result in a strong energy barrier that the upcoming dislocations need to overcome, and meanwhile this behavior is responsible for the severe periodical fluctuation of plastic stress flow in Fig. 5(a). Non-symmetrical stacking fault intersections are observed in the nanopillars of 1YSTZ and 2YSTZ, as shown in Figs. 7(b) and 7(c). More dislocation locks form in 1YSTZ nanopillar. In 2YSTZ nanopillar, although two dislocations on different slip planes meet with each other, the generated barrier is not as strong as the one observed in pure zirconia or 1YSTZ nanopillar. This is due to the formation of secondary slip planes that slightly tilts to the loading direction, which is also observed in 3YSTZ and 4YSTZ nanopillars [Figs. 7(d) and 7(e)].

It is worth to emphasis that to maintain the charge neutrality, the addition of $Y_2O_3$ will cause oxygen vacancies (half amount of $Y^{3+}$). It was observed in metallic systems[46] that dislocations act as rapid diffusion path for vacancies. Hence, it is reasonable to infer that in our current study the oxygen vacancies act as local weak points to facilitate the dislocation motion. In addition, dislocation crossing is detected in 3YSTZ [Fig. 7(d)], which indicates a much faster energy release than dislocation locking and consequently reduces the strength of the nanopillar. In comparison, neat primary slip plane and more secondary slip planes are observed in 4YSTZ nanopillar [Fig. 7(e)].

To study the composition effect on phase transformation, compression simulations of $[01\bar{1}]$-oriented YSTZ nanopillars are carried out. The obtained stress-strain curves in Fig. 5(b) indicate that by increasing the amount of the stabilizer ($Y_2O_3$), the strength of nanopillars decreases linearly [Fig. 6(a)], which is similar to the case of composition effect on dislocation migration [Fig. 5(a)]. Particularly, it is noted from Fig. 6(b) that the yield strain maintains the same value when composition is less than 2.0 mol. %, but it increases sharply as the yttria concentration increases from 2.0 mol. % to 3.0 mol. %. The atomistic configurations of the nanopillars at the strain of 3.5%, as shown in Figs. 7(f)–7(j), imply that the nanopillars with different compositions show different phase transformation behaviors. In pure zirconia nanopillar, although the initially transformed new phase band tilts to the (010) top/bottom surfaces with an angle of ~9°, with continuation

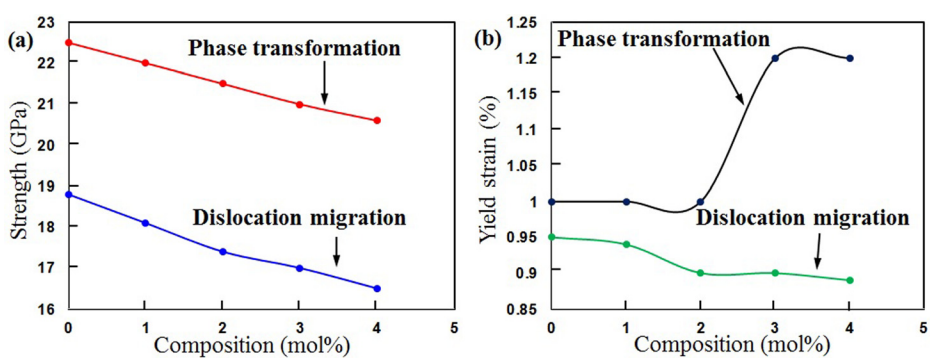


FIG. 6. Relationships of (a) strength versus composition and (b) yield strain versus composition for nanopillars with dislocation and phase transformation mediated deformation.

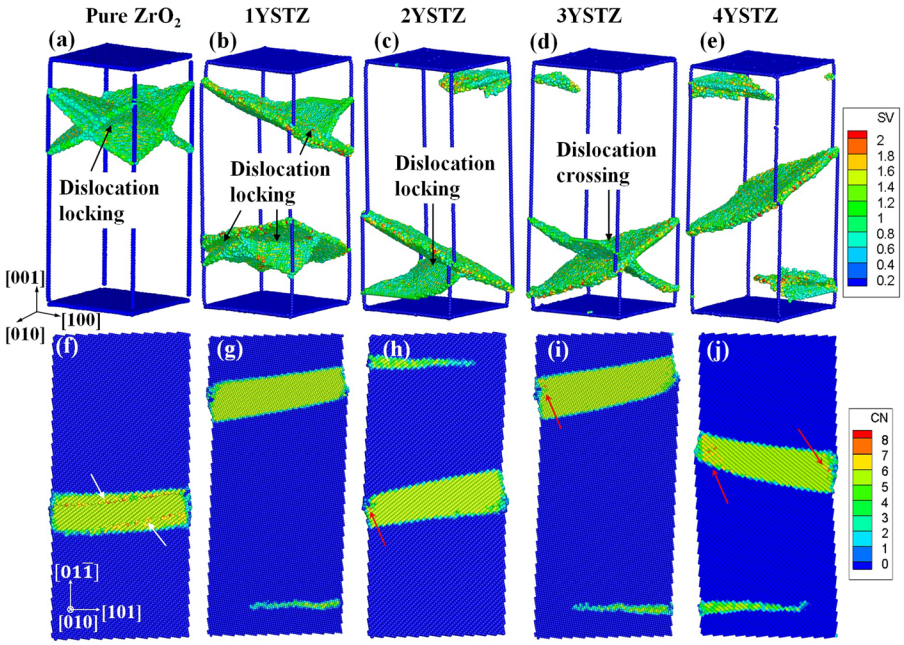


FIG. 7. (a)–(e) 3-D atomistic snapshots of the deformed [001]-oriented nanopillars with different amount of $Y_2O_3$ at the compressive strain of 1.0% (atoms are colored by slip vector). (f)–(j) atomistic snapshots of the deformed $[01\bar{1}]$-oriented nanopillars with different amount of $Y_2O_3$ at the strain of 3.5% (atoms are colored by CN).

of loading, the extension of original transformed monoclinic phase band is suppressed, then new phase transformation occurs with a different tilt angle, and finally makes the overall new phase band almost parallel to the (010) top/bottom surfaces [Fig. 7(f)]. Clear tilted boundaries can be identified after compression, as indicated by white arrows in Fig. 7(f). In addition, in the pure tetragonal nanopillar, one can notice that no secondary region of new phase forms, which is a significant different character with respect to YSTZ nanopillars. Considering the involvement of oxygen vacancies due to the introduction of $Y_2O_3$ into zirconia, it seems that oxygen vacancies accelerate $t \rightarrow m$ phase transformation compared to the pure tetragonal zirconia, and this is responsible for the high strength of pure zirconia in Fig. 5(b). Meanwhile, the role of oxygen vacancies can be used to explain the observed decrease of strength in YSTZ nanopillars with the increase of yttria concentration.

In 1YSTZ, 2YSTZ, 3YSTZ, and 4YSTZ nanopillars [Figs. 7(g)–7(j)], the originally transformed monoclinic phase band expands in a way to keep a tilted angle of $\sim 9^\circ$ to the (010) top/bottom surfaces. Besides, secondary phase transformation regions are observed to form at the top/bottom of the nanopillars to assist energy release, which leads to a lower plastic stress than pure $ZrO_2$, as can be seen in Fig. 5(b). Moreover, it is noticed that with increasing the amount of $Y_2O_3$, more amorphous phase is observed near the surface corrugation region of the transformed monoclinic phase, as indicated by red arrows in Fig. 7(j). Such phenomenon demonstrates that oxygen vacancies play another role to make the transformed monoclinic phase become unstable.

## IV. CONCLUSIONS

In conclusion, the effects of nanopillar specimen size and $Y_2O_3$ concentration on dislocation migration and phase transformation and consequently on mechanical properties of YSTZ nanopillars were studied. Dislocation motion was noticed to be interrupted under a critical size value between 12 and 16 nm, which leads to "smaller is stronger" phenomenon. $t \rightarrow m$ phase transformation dominated YSTZ nanopillars exhibit a strong size effect on mechanical properties. The strength of YSTZ was observed to reduce with the decrease of nanopillar size, i.e., "larger is stronger," due to the relatively large ratio of transformed monoclinic phase to the remaining tetragonal phase in the small-sized YSTZ nanopillar. Furthermore, $Y_2O_3$ concentration also showed significant effect on dislocation propagation and phase transformation. Oxygen vacancies, which were created by addition of stabilizer ($Y_2O_3$), acted as local weak points to facilitate dislocation motion. Meanwhile, they play roles of facilitating $t \rightarrow m$ phase transformation and also promoting the unstability of transformed monoclinic phase from the corrugation area. The strength of YSTZ nanopillar decreased linearly with the increase of $Y_2O_3$ content. Overall, our simulation results indicated that by suitable controlling the size and composition of YSTZ nanopillar, dislocation migration can be inhibited to reach higher yield strain and strength; on the other hand, phase transformation can be facilitated to achieve possible shape memory properties.

## ACKNOWLEDGMENTS

The authors are grateful for computer time allocation provided by the Extreme Science and Engineering Discovery Environment (XSEDE), Award No. TG-DMR140008.

[1]P. Mercera *et al.*, "Stabilized tetragonal zirconium oxide as a support for catalysts: Evolution of the texture and structure on calcination in static air," Appl. Catal. **78**(1), 79–96 (1991).
[2]M. Mamivand *et al.*, "Phase field modeling of the tetragonal-to-monoclinic phase transformation in zirconia," Acta Mater. **61**(14), 5223–5235 (2013).
[3]M. Mamivand, M. Asle Zaeem, and H. El Kadiri, "Phase field modeling of stress-induced tetragonal-to-monoclinic transformation in zirconia and its effect on transformation toughening," Acta Mater. **64**, 208–219 (2014).
[4]M. Mamivand, M. Asle Zaeem, and H. El Kadiri, "Shape memory effect and pseudoelasticity behavior in tetragonal zirconia polycrystals: A phase field study," Int. J. Plast. **60**, 71–86 (2014).

[5]J. Chevalier *et al*., "The tetragonal-monoclinic transformation in zirconia: Lessons learned and future trends," J. Am. Ceram. Soc. **92**(9), 1901–1920 (2009).
[6]N. Zhang and M. Asle Zaeem, "Competing mechanisms between dislocation and phase transformation in plastic deformation of single crystalline yttria-stabilized tetragonal zirconia nanopillars," Acta Mater. **120**, 337–347 (2016).
[7]X. M. Zeng *et al*., "Crystal orientation dependence of the stress-induced martensitic transformation in zirconia-based shape memory ceramics," Acta Mater. **116**, 124–135 (2016).
[8]N. Zhang *et al*., "Deformation mechanisms in silicon nanoparticles," J. Appl. Phys. **109**(6), 063534 (2011).
[9]S. M. Han *et al*., "Size effects on strength and plasticity of vanadium nanopillars," Scr. Mater. **63**(12), 1153–1156 (2010).
[10]M. D. Uchic *et al*., "Application of micro-sample testing to study fundamental aspects of plastic flow," Scr. Mater. **54**(5), 759–764 (2006).
[11]J. Diao *et al*., "Atomistic simulations of the yielding of gold nanowires," Acta Mater. **54**(3), 643–653 (2006).
[12]C. Frick *et al*., "Size effect on strength and strain hardening of small-scale [111] nickel compression pillars," Mater. Sci. Eng.: A **489**(1), 319–329 (2008).
[13]B. Schuster *et al*., "Microcompression of nanocrystalline nickel," Appl. Phys. Lett. **88**(10), 103112 (2006).
[14]X. W. Gu *et al*., "Size-dependent deformation of nanocrystalline Pt nanopillars," Nano Lett. **12**(12), 6385–6392 (2012).
[15]X. Chen and A. Ngan, "Specimen size and grain size effects on tensile strength of Ag microwires," Scr. Mater. **64**(8), 717–720 (2011).
[16]N. L. Okamoto *et al*., "Specimen-and grain-size dependence of compression deformation behavior in nanocrystalline copper," Int. J. Plast. **56**, 173–183 (2014).
[17]M. D. Uchic *et al*., "Sample dimensions influence strength and crystal plasticity," Science **305**(5686), 986–989 (2004).
[18]J. Biener *et al*., "Size effects on the mechanical behavior of nanoporous Au," Nano Lett. **6**(10), 2379–2382 (2006).
[19]J. R. Greer and W. D. Nix, "Nanoscale gold pillars strengthened through dislocation starvation," Phys. Rev. B **73**(24), 245410 (2006).
[20]F. Östlund *et al*., "Brittle-to-ductile transition in uniaxial compression of silicon pillars at room temperature," Adv. Funct. Mater. **19**(15), 2439–2444 (2009).
[21]T. Chraska, A. H. King, and C. C. Berndt, "On the size-dependent phase transformation in nanoparticulate zirconia," Mater. Sci. Eng.: A **286**(1), 169–178 (2000).
[22]A. Lai *et al*., "Shape memory and superelastic ceramics at small scales," Science **341**(6153), 1505–1508 (2013).
[23]Z. Du *et al*., "Size effects and shape memory properties in $ZrO_2$ ceramic micro-and nano-pillars," Scr. Mater. **101**, 40–43 (2015).
[24]E. Camposilvan and M. Anglada, "Size and plasticity effects in zirconia micropillars compression," Acta Mater. **103**, 882–892 (2016).
[25]J. San Juan and M. Nó, "Superelasticity and shape memory at nano-scale: Size effects on the martensitic transformation," J. Alloys Compd. **577**, S25–S29 (2013).
[26]H. Brinkman, W. Briels, and H. Verweij, "Molecular dynamics simulations of yttria-stabilized zirconia," Chem. Phys. Lett. **247**(4-6), 386–390 (1995).
[27]S. Fabris, A. T. Paxton, and M. W. Finnis, "A stabilization mechanism of zirconia based on oxygen vacancies only," Acta Mater. **50**(20), 5171–5178 (2002).
[28]U. Messerschmidt *et al*., "Plastic deformation of zirconia single crystals: A review," Mater. Sci. Eng.: A **233**(1-2), 61–74 (1997).
[29]A. Bravo-Leon *et al*., "Fracture toughness of nanocrystalline tetragonal zirconia with low yttria content," Acta Mater. **50**(18), 4555–4562 (2002).
[30]E. Zapata-Solvas *et al*., "High temperature creep behaviour of 4 mol% yttria tetragonal zirconia polycrystals (4-YTZP) with grain sizes between 0.38 and 1.15 $\mu$m," J. Eur. Ceram. Soc. **27**(11), 3325–3329 (2007).
[31]F. Wakai, S. Sakaguchi, and Y. Matsuno, "Superplasticity of yttria-stabilized tetragonal $Zr_2O$ polycrystals," Adv. Ceram. Mater. **1**(3), 259–263 (1986).
[32]J. Kondoh *et al*., "Yttria concentration dependence of tensile strength in yttria-stabilized zirconia," J. Alloys Compd. **365**(1), 253–258 (2004).
[33]M. Trunec and Z. Chlup, "Higher fracture toughness of tetragonal zirconia ceramics through nanocrystalline structure," Scr. Mater. **61**(1), 56–59 (2009).
[34]T. Masaki and K. Sinjo, "Mechanical properties of highly toughened $ZrO_2{\cdot}Y_2O_3$," Ceram. Int. **13**(2), 109–112 (1987).
[35]J. Zhu *et al*., "Effect of surface composition of yttrium-stabilized zirconia on partial oxidation of methane to synthesis gas," J. Catal. **230**(2), 291–300 (2005).
[36]S. Wu and S. Yang, "Effect of composition on transformation temperatures of Ni–Mn–Ga shape memory alloys," Mater. Lett. **57**(26), 4291–4296 (2003).
[37]S. Prokoshkin *et al*., "Alloy composition, deformation temperature, pressure and post-deformation annealing effects in severely deformed Ti–Ni based shape memory alloys," Acta Mater. **53**(9), 2703–2714 (2005).
[38]N. Zhang and Y. Chen, "Nanoscale plastic deformation mechanism in single crystal aragonite," J. Mater. Sci. **48**(2), 785–796 (2013).
[39]N. Zhang *et al*., "Nanoscale toughening mechanism of nacre tablet," J. Mech. Behav. Biomed. Mater. **53**, 200–209 (2016).
[40]X. Li and B. Hafskjold, "Molecular dynamics simulations of yttrium-stabilized zirconia," J. Phys.: Condens. Matter **7**(7), 1255 (1995).
[41]S. Plimpton, "Fast parallel algorithms for short-range molecular dynamics," J. Comput. Phys. **117**(1), 1–19 (1995).
[42]L. Verlet, "Computer "experiments" on classical fluids. I. Thermodynamical properties of Lennard-Jones molecules," Phys. Rev. **159**(1), 98 (1967).
[43]W. G. Hoover, "Canonical dynamics: Equilibrium phase-space distributions," Phys. Rev. A **31**(3), 1695 (1985).
[44]U. Messerschmidt, B. Baufeld, and D. Baither, "Plastic deformation cubic zirconia single crystals," Key Eng. Mater. **153–154**, 143–182 (1998).
[45]R. H. Hannink, P. M. Kelly, and B. C. Muddle, "Transformation toughening in zirconia-containing ceramics," J. Am. Ceram. Soc. **83**(3), 461–487 (2000).
[46]K. Otsuka *et al*., "Dislocation-enhanced ionic conductivity of yttria-stabilized zirconia," Appl. Phys. Lett. **82**(6), 877–879 (2003).